Aperture Antenna Modelling by a Finite Number of Elemental Dipoles from Truncated Spherical Field Measurement: Experimental Investigation

M. Serhir(*), J.M. Geffrin(+), A. Litman(+) ,N. Ribiere-Tharaud(*) and P. Besnier(#)

* *DRE, Laboratoire des Signaux et Systèmes (UMR 8506 : CNRS Supelec-Univ. Paris-Sud 11), SUPELEC, 3 Rue Joliot-Curie, 91192 Gif-sur-Yvette, Cedex France*

mohammed.serhir@supelec.fr, nicolas.ribiere-tharaud@supelec.fr

\+ *Institut FRESNEL Universités Aix-Marseille, Ecole Centrale Marseille, CNRS, Institut Fresnel, Campus de Saint Jérôme, 13013 Marseille France*

jean-michel.geffrin@fresnel.fr, amelie.litman@fresnel.fr

\# *INSA de Rennes/IETR 20, avenue des Buttes de Coësmes, 35043 Rennes cedex, France*

philippe.besnier@insa-rennes.fr

***Abstract*— A method to determine a distribution of a finite number of elementary dipoles that reproduce the radiation behaviour of the antenna under test (AUT) from truncated spherical field measurements is proposed. It is based on the substitution of the actual antenna by a finite number of equivalent infinitesimal dipoles (electric and magnetic), distributed over the antenna aperture. This equivalent set of elementary dipoles is optimized using the transmission coefficient involving the spherical wave expansion of the measured field and using an appropriate matching method. Once the current excitation of each dipole is known, the radiated field of the antenna at different distances can be rapidly determined. The reliability and the accuracy of the method are shown using experimental data issued from the measurement of an X-band horn antenna, in two different measurement setups.**

I. Introduction

For most of the commercial antennas, the geometric parameters and the material characteristics may not be accessible or may even be unknown. Measurements, such as near-field (NF) techniques, are therefore the only way to determine accurately the radiation characteristics of the antenna. The issue is to derive from these measurements the radiation pattern of the antenna in its real environment.

In this paper, we propose a hybrid three-step approach. Firstly, the radiation pattern of the antenna under test is measured in a completely controlled environment (anechoic chamber). Secondly, from these measurements, a simple equivalent model is achieved in terms of elementary equivalent sources that reproduce the antenna radiation pattern. Finally, this equivalent model is incorporated into a commercial electromagnetic (EM) algorithm to assess the behaviour of the modelized antenna in different environments (operating conditions).

In the literature, many authors have proposed different strategies where they determine currents/charges distributions that radiate an electromagnetic field matching the AUT radiation. In [1-3], the authors used the Genetic Algorithm (GA) technique to substitute the AUT by a set of infinitesimal dipole sources. The infinitesimal dipoles have been selected due to their implementation simplicity in any EM code, and the GA demonstrates its ability to figure out the type (electric or magnetic), the position, the orientation and the excitation of each dipole. The limitation of this method appears when dealing with electrically large structures, which require a large number of equivalent dipoles, as well as convergence issues and prohibitive CPU computing time.

In [4] the authors have developed a modelling technique, based on the equivalence principle. The AUT is substituted by a set of equivalent dipoles distributed over the minimum sphere circumscribing the antenna (closed surface). The excitations of the antenna equivalent dipoles are derived from the AUT transmission coefficients. Computations with EM simulation data illustrate the accuracy of the method. Nevertheless, these equivalent sources distribution is not optimum for large radiating structures, particularly, for aperture antennas (horn antennas). The number of equivalent sources grows considerably when the sources are distributed over the antenna minimum sphere.

In the present paper, an improvement of the analysis of [4] is presented. The antenna equivalent current sources are placed over a planar surface with finite extent in front of the antenna aperture (S_{equi}) and only tangential dipoles are considered. For this purpose, spherical field measurement data is used to determine the spherical wave expansion (SWE) of the horn antenna radiated field. Then, taking into account the antenna geometrical a priori information, and by adopting a convenient equivalent sources spatial distribution over the planar surface, the SWE of the antenna radiated field is written in terms of tangential electric and magnetic dipoles placed over the antenna aperture wherein the excitations of the dipoles are correlated to the antenna transmission coefficients.

The most significant aspect studied in the present paper is the reliability and the accuracy of the method when using experimental data issued from the measurement of a real antenna (horn antenna) in the far-field region.

To asses the overall procedure, the radiation pattern of an X-band horn antenna has been measured over a truncated sphere using a single probe spherical range measurement in the large anechoic chamber of the Institut Fresnel [5]. Once the equivalent model is defined, we compute the radiation pattern at a different distance. In particular, the estimated pattern is compared to another set of measurements performed this time with a single probe planar measurement setup, which corresponds to the new anechoic chamber of the Institut Fresnel. A comparison between the SWE and the proposed modelling technique in terms of computation time is presented.

The paper is constructed as follows: In Section II, following a review of the spherical wave expansion formulation, the basis of the proposed technique is detailed. Section III presents the modelling process applied to the X-band horn antenna radiating at the frequency of 12 GHz. In order to illustrate the robustness of the proposed modelling technique we use truncated experimental measurement data to validate the efficiency of the method. The setups, as well as the measurement procedure, are described in section III. Concluding remarks are outlined in section IV. All theoretical quantities are expressed in the S.I. rationalized unit system with e^{-jwt} time dependence

II. CONSTRUCTION OF THE EQUIVALENT MODEL

The proposed modelling technique aims to find the excitation of a given number (L_{source}) of equivalent current sources that reproduce the antenna radiation pattern. In particular for a horn antenna, these sources are placed over the planar surface representing the horn aperture S_{equi} (Fig. 1). We make use of the theoretical development, detailed in [4], regarding the new spatial distribution of the equivalent sources adopted in this work.

We define a current source as the combination of four tangential co-localized short dipoles: 2 electric ones and 2 magnetic ones. The i[th] current source (for $1 \le i \le L_{source}$), is associated to a coordinate system $(o_i, \vec{x_i}, \vec{y_i}, \vec{z_i})$, where the origin coincides with the position of this source in the AUT global coordinate system $(O, \vec{X}, \vec{Y}, \vec{Z})$. The aim of this work is to use the AUT transmission coefficients to determine the excitation of the equivalent sources. These coefficients are determined from truncated measurement data in contrast to [4], where they were computed from a complete sphere of synthesised data (using a simulation software).

A. Spherical wave expansion

The SWE of the radiated field $\vec{E}_{AUT}$ in the spherical coordinate system associated to the global coordinate system $(O, \vec{X}, \vec{Y}, \vec{Z})$, where the origin $O(0,0,0)$ coincides with the centre of the measurement sphere (Fig. 1), is expressed in terms of truncated series of spherical vector wave functions [6] as

$$\vec{E}_{AUT}(\vec{r}) = \frac{k}{\sqrt{\eta}} \sum_{s=1}^{2} \sum_{n=1}^{N_{tr}} \sum_{m=-n}^{m=n} Q_{s,m,n} \vec{F}^{(3)}_{s,m,n}(\vec{r}) = \frac{k}{\sqrt{\eta}} \sum_{j=1}^{J_{\max}} Q_j \vec{F}^{(3)}_j(\vec{r}), \quad (1)$$

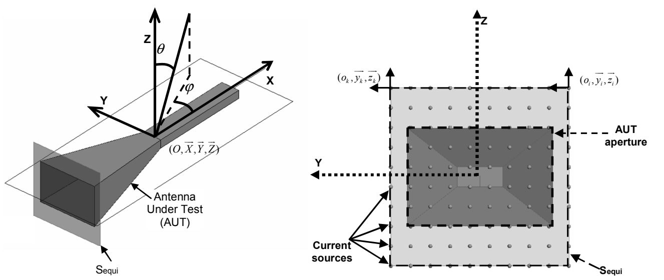

Fig. 1. Original horn antenna (left) and the equivalent current sources distribution over the equivalent surface S_{equi} (right).

where $N_{tr} = [kr_{\min}] + 10$ and k corresponds to the wave number, $\eta = \sqrt{\varepsilon/\mu}$ the intrinsic admittance of the medium, $Q_{s,m,n}$ are the spherical wave coefficients (transmission coefficients), and $\vec{F}^{(3)}_{s,m,n}(\vec{r})$ represent the power-normalized spherical vector wave functions. In [7-8] truncated near-field measurement data has been shown to be sufficient to calculate the Q_j coefficients. Once the Q_j are determined, the field outside the measurement sphere is completely characterized by Eq.(1).

Our aim is to take advantage of the compactness of the SWE expression for the field radiated by a short dipole ($N_{tr} = 1$ for electric or magnetic dipole) and to relate the field radiated by an antenna described by $J_{\max}$ spherical vector wave functions to the set of infinitesimal dipoles using translational and rotational addition theorems.

B. Short dipole excitation

In what follows, the superscripts 'e' and 'm' stand for the electric and magnetic dipoles, respectively. The subscripts 'y' and 'z' denote $\vec{y}$, $\vec{z}$ polarized dipoles, respectively. The subscript 'i' designates the i[th] current source located at the position $o_i(x_i, y_i, z_i)$ in $(O, \vec{X}, \vec{Y}, \vec{Z})$.

The field $\vec{E}^{e,z}_i$ radiated by an infinitesimal $\vec{z}$-directed electric dipole located at the origin of $(o_i, \vec{x_i}, \vec{y_i}, \vec{z_i})$ is expressed in the spherical coordinate system $\vec{r_i}(r_i, \theta_i, \varphi_i)$ associated with $(o_i, \vec{x_i}, \vec{y_i}, \vec{z_i})$ as

$$\overrightarrow{E^{e,z}_{i}}(\vec{r_i}) = \frac{k}{\sqrt{\eta}} \alpha^{e,z}_{i} \overrightarrow{F^{(3)}_4}(\vec{r_i}) \quad \text{, with } \alpha^{e,z}_i = -\frac{k}{\sqrt{6\eta\pi}} I^{e,z}_i l, \quad (2)$$

In the global spherical coordinate system $\vec{r}(r, \theta, \varphi)$ associated with $(O, \vec{X}, \vec{Y}, \vec{Z})$ we have

$$\overrightarrow{F^{(3)}_4}(\vec{r}) = \sum_{j=1}^{J_{\max}} A^{e,z}_{j,i} \vec{F}^{(3)}_j(\vec{r}) \qquad (3)$$

From (2) and (3) it follows that the field in the global spherical coordinate system $\vec{r}(r, \theta, \varphi)$ is given by

$$\overrightarrow{E^{e,z}_i}(\vec{r}) = \frac{k}{\sqrt{\eta}} \alpha^{e,z}_i \sum_{j=1}^{J_{\max}} A^{e,z}_{j,i} \vec{F}^{(3)}_j(\vec{r}) \qquad (4)$$

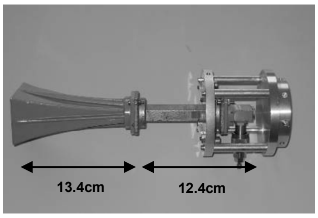

Fig. 2. The AUT description: an X-band horn antenna with the exciting wave-guide

Detailed formulations and expressions for $\vec{x}$ and $\vec{y}$ -dipoles are provided in [4]. Accordingly, the ith current source is composed of 4 co-localized tangential dipoles, this will be characterized by 4 transmission coefficients $\alpha_i^{e,y}$, $\alpha_i^{m,y}$, $\alpha_i^{e,z}$, $\alpha_i^{m,z}$. These coefficients are proportional to the dipoles length 'l' and to the current excitations $I_i^{e,y}$, $I_i^{m,y}$, $I_i^{e,z}$, $I_i^{m,z}$. We associate to the ith current source the row vector $\left[S_i\right]$ where,

$$\begin{aligned}\left[S_i\right] &= \left[\alpha_i^{e,y}, \alpha_i^{m,y}, \alpha_i^{e,z}, \alpha_i^{m,z}\right] \ \text{in}\,(o_i, \overrightarrow{x_i}, \overrightarrow{y_i}, \overrightarrow{z_i}) \\ &= \left[\alpha_i^{e,y} A_{j,i}^{e,y}, \alpha_i^{m,y} A_{j,i}^{m,y}, \alpha_i^{e,z} A_{j,i}^{e,z}, \alpha_i^{m,z} A_{j,i}^{m,z}\right]^{1 \le j \le J_{\max}} \\ &\qquad \text{in}\,(O, \vec{X}, \vec{Y}, \vec{Y})\end{aligned} \quad (5)$$

The coefficients $A_{j,i}^{e,y}$, $A_{j,i}^{m,y}$, $A_{j,i}^{e,z}$, $A_{j,i}^{m,z}$ are described in the Appendix of [4].

C. *Antenna modelling method*

In order to determine the excitation of each elemental dipole composing the equivalent model, we have to define the adequate matching method. This can only be done in the global coordinate system. This is why we have used translational and rotational addition theorems [6, 9, 10] to express the field radiated by the ith current source located at $o_i(x_i, y_i, z_i)$ in the antenna global coordinate system $(O, \vec{X}, \vec{Y}, \vec{Z})$.

Then, the superposition of all the L_{source} current sources field $\vec{E}_{\mathrm{mod}}(\vec{r})$ expressed in $(O, \vec{X}, \vec{Y}, \vec{Z})$ is identified with $\vec{E}_{AUT}$. In the same way as [4] we have to solve the linear equations

$$\mathbf{AX} = \mathbf{Q}. \quad (6)$$

where, $\mathbf{A} = \left[A_{j,i}^{e,y}, A_{j,i}^{m,y}, A_{j,i}^{e,z}, A_{j,i}^{m,z}\right]_{1 \le i \le L_{source}}^{1 \le j \le J_{\max}}$, $\mathbf{X} = \left[S_1 \ldots \quad S_{L_{source}}\right]^{\mathrm{T}}$ and $\mathbf{Q} = \left[Q_1 \ldots \quad Q_{J_{\max}}\right]^{\mathrm{T}}$. The superscript 'T' denotes the matrix transpose.

The lsqr routine from MatLab (least square data fit) [11] has been used to solve the over-determined matrix equation ($4 \times L_{source} \le J_{\max}$). Once Equation (6) is solved, the equivalent model characterization is finalized and each current excitation $\left(I_i^{e,y}, I_i^{m,y}, I_i^{e,z}, I_i^{m,z}\right)_{1 \le i \le L_{source}}$ is fully computed.

III. Results

To illustrate the effectiveness of the proposed methodology, the modelling process is applied to a commercial X-band horn antenna, (Fig. 2) operating at the frequency of 12 GHz. The waveguide dimensions are 124 mm x 23 mm and the aperture size is 73.5 mm x 50 mm (3λx2λ). The associated minimum sphere circumscribing the antenna has a radius of $r_{\min} \simeq 175mm$ (7λ). This antenna is measured using the spherical field system in the anechoic chamber of the Centre Commun des Resources Micro-ondes of Marseille (CCRM) managed for this topic by Institut Fresnel researchers, which is presented in Fig. 3 [6]. The tangential complex components of the electric field (E_θ, E_φ) of this antenna have been measured at the distance $R_{meas} = 1.79m = 71.6\lambda$. To carry out the equivalent current sources model, the measurement data are collected over a truncated spherical surface ($15° \le \theta \le 165°, 105° \le \varphi \le 357°$). The field sampling is of 3° both in θ and φ coordinates, with 51x51 measurement points.

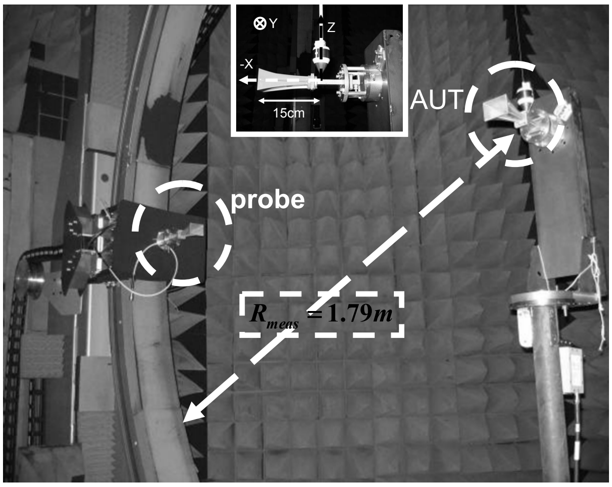

Fig. 3. Measurement setup using the single probe spherical near field range at CCRM (left). Description of the measured horn antenna (AUT) position in the measurement coordinate system (right).

The measurement data matrix is completed (with null field values) in order to fulfil the measurement over a sphere $0 \le \theta \le 180°, 0° \le \varphi \le 357°$. Based on these data and using the matrix method [7] we compute the antenna transmission coefficients. These are presented in Fig. 4. The SWE is truncated at $N_{tr} = \left[kr_{\min}\right] + 10 = 54$, such that $J_{\max} = 2 \times 54 \times 56 = 6048$ transmission coefficients are considered for the current configuration.

The AUT equivalent model is composed of 10x10 current sources separated by 0.4λ. These sources are chosen to be distributed uniformly over a planar domain S_{equi} of size $90mm \times 90mm$ positioned at the antenna aperture plane $x \simeq -150mm$ (Fig. 3). From a theoretical point of view, the aperture plane should be infinite. However, it is possible to truncate it as the radiated power of the antenna, and consequently, the equivalent dipoles, is concentrated in a finite region in front of the antenna aperture.

Once the transmission coefficients of the antenna are known and the equivalent current sources positions defined, we solve Eq.6 and we compute the current excitation of each

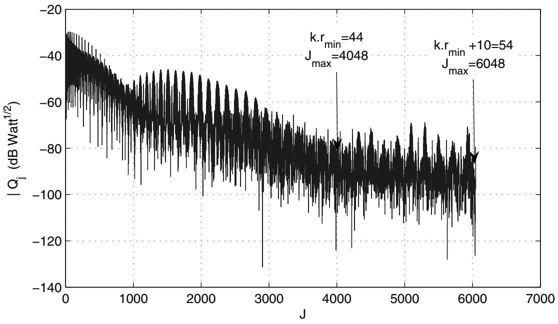

fig.4 Magnitude of the AUT transmission coefficients calculated using the measurement data collected over the spherical surface $R_{meas} = 1.79m$, for $15 \le \theta \le 165°$ and $105° \le \varphi \le 255°$.

dipole. Thereafter, we rapidly calculate the E-field at different distances.

The E-field radiated by the AUT equivalent model is compared to the actual antenna radiation pattern in the measurement area $15° \le \theta \le 165°, 105° \le \varphi \le 357°$ in Fig.5 at the measurement distance. The measured field and the field obtained from the equivalent model are in a good agreement. In addition, the radiation pattern obtained from the equivalent model fits very well with the one resulted from the SWE method as presented in Fig.6. Also, as shown in Fig.5, the field radiated by the equivalent model tends to cancel the ripples observed in the measured field. These ripples are principally caused by measurement errors as for example: multiple reflections between the AUT and the measurement probe, the interaction between the antenna and its mounting system….

In Fig. 7 we present the equivalent dipoles distribution over S_{equi} . As it can be seen the region where the magnitude of the equivalent dipoles is significant coincides with the horn aperture (dashed rectangle). The horn antenna being off-centred during the measurement, this can justify the fact that we have considered an equivalent aperture (S_{equi}), whose dimensions are greater than the horn actual aperture. Nevertheless, the equivalent dipoles magnitude is consistent with the actual E-field in the aperture of the antenna, since the significant equivalent dipoles are concentrated in the aperture area (dashed rectangle).

The performances modelling procedure is evaluated by comparing the equivalent model E-fields with the actual radiation pattern over a line ($x = -45cm,\ -40cm \le y \le 40cm,$ $z = 0$) at a distance of 30cm from the horn antenna aperture which is closer than the measurement made for the equivalent model determination (1.79m). To achieve this measurement, we have exploited the new measurement setup of the Institut Fresnel which consists in a single probe planar measurement system in an anechoic environment (Fig.8).

The planar scanner has a total dual scan length of 2.1m in X and Y direction placed in an anechoic environment. The same horn antenna is used in the transmit mode. The probe, which is mounted on one of the two carriages of the linear scanner,

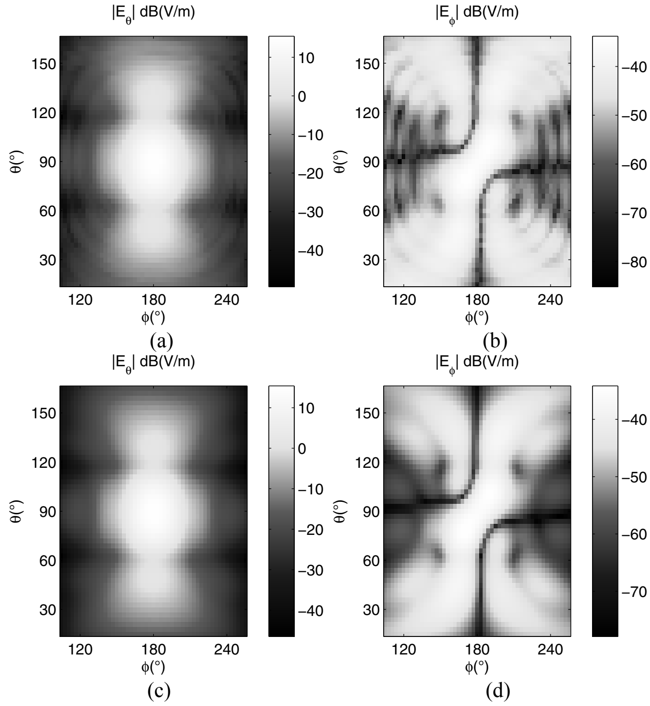

Fig.5. Magnitude of the E-field components E_θ and E_φ in dB (V/m) at the measurement distance $R_{meas} = 1.79m$. In (a) and (b) the measured field radiated by the actual horn antenna and in (c) and (d) the field radiated by the antenna equivalent model determined using truncated measurements.

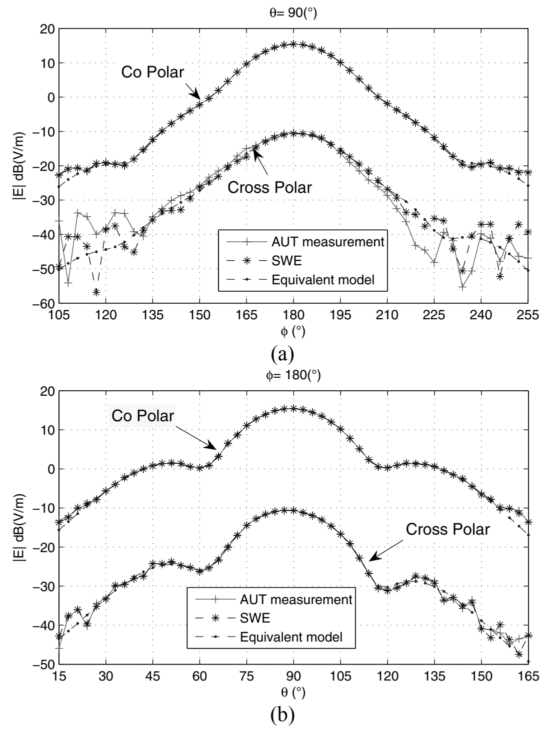

Fig.6. Comparison of co-polarized and cross-polarized components of the fields at the measurement distance $R_{meas} = 1.79m$. The comparison includes: the AUT measurement, the field calculated using the SWE and the field radiated by the equivalent model based on truncated spherical measurement. (a) for $\theta = 90°$ and (b) for $\varphi = 180°$.

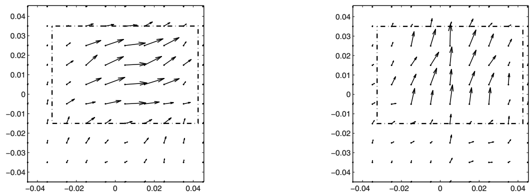

Fig.7. The magnitude of the equivalent dipoles distributed over the equivalent surface (S_{equi}). (left) Magnetic dipoles. (right) Electric dipoles. The dashed rectangle represents the AUT actual aperture.

consists of an open ended wave guide. The probe is connected to a vector network analyser (VNA) and the magnitude and the phase of the antenna radiated field are measured. A computer monitors the probe displacement over the line in front of the antenna and acquires the data provided by the VNA.

In Fig.8 we present the Ez field radiated by the AUT equivalent model compared to the measured Ez field and the field estimated using the SWE method over a line at a distance of 30cm from the aperture. As it can be seen, the agreement is excellent. In addition, we present in Fig. 8 the computation time needed to calculate Ez at the measurement distance (30 cm from the AUT aperture). Once the equivalent model is fully defined the E field is rapidly estimated at different distances, faster than using the SWE. This is due to the fact that, the number of equivalent dipoles is smaller than the number of the AUT transmission coefficients.

In addition, implementing the equivalent model in an EM code, one is able to calculate the E-field propagation properties in complex and inhomogeneous environments. As an example, one can study the antenna radiation pattern through an interface between the free space and a homogeneous media.

IV. CONCLUSION

The presented method aims to substitute the measured AUT by a set of infinitesimal dipoles regularly distributed over the antenna aperture surface, simply from the knowledge of the measured field over a truncated spherical surface. Based on the orthogonal properties of the spherical vector wave functions, the presented matching method has been shown to be a convenient tool to define a set of elementary structures (with $N_{tr} = 1$) from the antenna transmission coefficients. We have shown from the presented example (X-band horn antenna) that from the collected tangential electric field, the equivalent principle can be applied to an equivalent planar surface of finite size. The equivalent model can reproduce rapidly the actual radiation pattern at different distances from the considered antenna. The overall procedure has been assessed by exploiting two different measurement systems, a spherical one and a planar one, both being in anechoic environments.

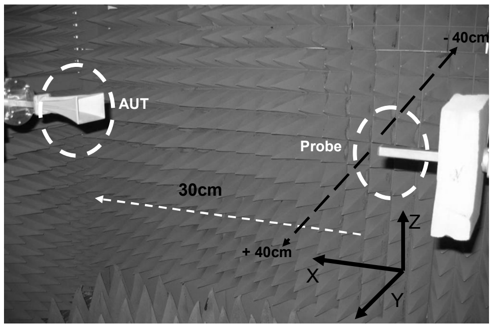

(a)

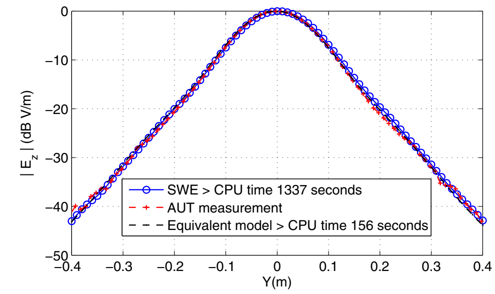

(b)

Fig.8. (a) Measurement setup using the single probe planar near field range at Institut Fresnel.(b) The magnitude of the Ez field measured at the distance of 30cm from the AUT aperture compared with the Ez fields calculated from the SWE and the simplified equivalent models.

REFERENCES

[1] J. R. Pérez and J. Basterrechea, “Antenna far-field pattern reconstruction using equivalent currents and genetic algorithms” Microwave Opt. Technol. Lett., Vol.42, No. 1, pp. 21-25, July 2004.

[2] T. S. Sijher and A.A. Kishk, “Antenna modeling by infinitesimal dipoles using genetic algorithms” Progress In Electromagnetics Research, PIER 52, pp. 225-254, 2005.

[3] Mikki, S.M.and Kishk, A.A “Theory and Applications of Infinitesimal Dipole Models for Computational Electromagnetics,” IEEE Transact. Antenna Propagat., Vol. 55, pp.1325 - 1337, May. 2007.

[4] M. Serhir, P. Besnier and M.Drissi, “An accurate equivalent behavioral model of antenna radiation using a mode-matching technique based on spherical near field measurements,” IEEE Transact. Antenna Propagat., Vol. 56, pp. 48-57, Jan. 2008.

[5] C. Eyraud, J. Geffrin, P. Sabouroux, P. C. Chaumet, H. Tortel, H. Giovannini, and A. Litman (2008), Validation of a 3D bistatic microwave scattering measurement setup, Radio Sci., 43, RS4018,

[6] J. E. Hansen, Spherical Near-Field Antenna Measurements. London, U.K.: Peregrinus, 1988.

[7] M. Mekki-Kaidi, D. Lautru, F. Bancet and V. Fouad Hanna, “A matrix inversion technique for the spherical modal decomposition field solution applied on the characterization of antenna in their environment,” Microwave Opt. Technol. Lett., Vol.41, No. 5, pp. 336-341, June 2004.

[8] Koivisto, P. and J. C. –E. Sten, “On the influence of incomplete radiation pattern data on the accuracy of a spherical wave expansion” Progress In Electromagnetics Research, PIER 52, pp. 185-204, 2005.

[9] A. R. Edmonds, Angular Momentum in Quantum Mechanics, 3rd ed. Princeton, NJ: Princeton Univ. Press, 1974.

[10] J. H. Bruning and Y. T. Lo, “Multiple scattering of EM waves by spheres, Part I – Multipole expansion and ray-optical solutions,” IEEE Trans. Antennas Propagat. Vol. Ap-19, pp. 378-390, May 1971.

[11] MatLab user’s guide.